

Single frequency Ti:sapphire laser with continuous frequency-tuning and low intensity noise by means of the additional intracavity nonlinear loss

Huadong Lu,* Xuejun Sun, Meihong Wang, Jing Su, and Kunchi Peng

State Key Laboratory of Quantum Optics and Quantum Optics Devices, Institute of Opto-Electronics, Shanxi University, Taiyuan, Shanxi 030006, China

*luhuadong@sxu.edu.cn

Abstract: A single frequency Ti:sapphire (Ti:S) laser with continuous frequency-tuning and low intensity noise is presented, in which an extra nonlinear (NL) loss crystal is placed inside the resonator instead of the traditional etalon locking system. When a NL crystal is inserted into a home-made Ti:S laser resonator, the single frequency laser of 1.27 W at 795 nm with a continuous frequency-tuning range of 48 GHz is realized under the pump level of 11.27 W and the intensity noise at the lower frequencies is successfully suppressed.

© 2014 Optical Society of America

OCIS codes: (140.3590) Lasers, titanium; (140.3560) Lasers, ring; (140.3570) Lasers, single-mode; (140.3600) Lasers, tunable.

References and links

1. Z. X. Xu, Y. L. Wu, L. Tian, L. R. Chen, Z. Y. Zhang, Z. H. Yan, S. J. Li, and H. Wang, "Long lifetime and high-fidelity quantum memory of photonics polarization qubit by lifting zeeman degeneracy," *Phys. Rev. Lett.* **111**(5), 240503 (2013).
2. X. J. Jia, Z. H. Yan, Z. Y. Duan, X. L. Su, H. Wang, C. D. Xie, and K. C. Peng, "Experimental realization of three-color entanglement at optical fiber communication and atomic storage wavelength," *Phys. Rev. Lett.* **109**, 253604 (2012).
3. H. D. Lu, J. Su, C. D. Xie, and K. C. Peng, "Experimental investigation about influences of longitudinal-mode structure of pumping source on a Ti:sapphire laser," *Opt. Express* **19**(2), 1344–1353 (2011).
4. <http://www.coherent.com/Products/index.cfm?846/MBR-Ring-Series>.
5. <http://www.spectra-physics.com/products/tunable-lasers/matisse/>.
6. S. Kobtsev, V. Baraoulya, and V. Lunin, "Ultra-narrow-linewidth combined CW Ti:sapphire/Dye laser for atom cooling and high-precision spectroscopy," *Proc. SPIE* **6451**, 64511U (2007).
7. <http://www.m2lasers.com/products/laser-systems/ti-sapphire-laser.aspx>.
8. K. I. Martin, W. A. Clarkson, and D. C. Hanna, "Self-suppression of axial mode hopping by intracavity second-harmonic generation," *Opt. Lett.* **22**(6), 375–377 (1997).
9. H. D. Lu, J. Su, Y. H. Zheng, and K. C. Peng, "Physical conditions of single-longitudinal-mode operation for high-power all-solid-state lasers," *Opt. Lett.* **39**(5), 1117–1120 (2014).
10. H. D. Lu, "Intracavity losses measurement of the Ti:sapphire laser with relaxation resonant oscillation frequency and output power," *Chin. J. Lasers* **40**(4), 0402002 (2013).

1. Introduction

All-solid-state continuous-wave (CW) single-frequency tunable Ti:sapphire (Ti:S) lasers with compact configuration and high efficiency have been extensively applied to high-sensitive laser

spectroscopy, quantum communications, high-precision interferometry and so on. Since the peak wavelength 795 nm of Ti:S corresponds to the D₁ line of rubidium, it is applied in quantum information protocols to implement the quantum storage [1]. Single-frequency 795 nm laser is also used as the pump source of multi-color entangled state generation system, which has potential application in the fiber quantum communication [2]. Recent years, since single-frequency Ti:S lasers are used in the experimental researches of laser cooling for atoms, more and more attentions have been focused on the continuous frequency-tuning ability and low intensity noise [3] of Ti:S lasers. Four commercial versions of continuous frequency tunable CW Ti:S lasers have been developed by Coherent [4], Spectra-Physics [5], Tekhnoscan Joint-Stock [6] and M-square companies [7], respectively. In all these laser products, in order to prevent the mode-hopping during the frequency-tuning, the peak of an etalon transmission curve is locked on the wavelength of the oscillating laser. Since the etalon-locking is the modulation locking, the modulation signal increases the intensity noise of Ti:S laser at the low frequencies, which is harmful for applications in quantum optics experiments and quantum information. In 1997, K. I. Martin [8] observed a large degree of suppression of the axial mode-hopping generated during the cavity-length tuning in a second-harmonic generation (SHG) process, and pointed out that was resulted from the unbalanced losses introduced by the SHG among the lasing mode and other nonlasing modes. On the basis of the theoretical analysis, they obtained frequency tuning range of 80 GHz for the doubled frequency in an intracavity SHG laser. In 2014, we theoretically and experimentally investigated the physical conditions of single-longitudinal-mode (SLM) operation for high-power all-solid-state lasers at a given oscillating frequency. By inserting a nonlinear (NL) crystal into the resonator, a stable SLM 1064 nm laser with the output power of 33.7 W and the optical-optical conversion efficiency of 44.9% were obtained [9], in which the issues of the frequency-tuning and intensity noise were not involved. Here, we extend the function of the intracavity NL loss to realize the continuous frequency-tuning and low intensity noise of the fundamental-wavelength laser. By means of the action of the intracavity NL loss, a laser with the continuous frequency-tuning and low intensity noise can be realized only by continuously scanning the length of the resonator without the use of any frequency-locking system.

2. Frequency-tuning principle

It has been demonstrated in [8] that when a NL crystal is placed in a laser resonator, the NL loss of the lasing mode is half of that of nonlasing modes and the loss difference between lasing and nonlasing modes is equal to the second-harmonic conversion efficiency. This result will apply to all nonlasing modes that fall within the phase-matching bandwidth for harmonic or sum-frequency generation. When the cavity length is progressively changed, the single-frequency would scan continuously without mode hopping until the gain of the lasing mode is lower than SHG conversion efficiency because of the frequency offset. At that point the mode closest to the gain line center would have a net gain higher than that of the lasing mode. A mode hop would occur to the mode near the line center. This frequency offset or the basic smooth frequency tuning range of the SLM laser is defined by:

$$\Delta\nu_{\max} = \frac{\Delta\nu_{\text{eff}}}{2} \sqrt{\frac{\eta}{\eta+L}} \quad (1)$$

where L is the linear loss including the round-trip cavity loss and the loss introduced by the transmission of the output coupler, but excluding the NL loss, η is the frequency-doubling conversion efficiency, and $\Delta\nu_{\text{eff}}$ is the effective gain linewidth. In principle, the maximal frequency-tuning range decided by the linear and NL losses, is the significant fraction of the laser gain linewidth. As usual, the effective gain linewidth is that of the gain medium. However, a birefringent filter or an etalon, which can contribute a frequency selectivity, is usually inserted into the resonant cavity to improve the stability of the SLM lasers. The effective linewidth with

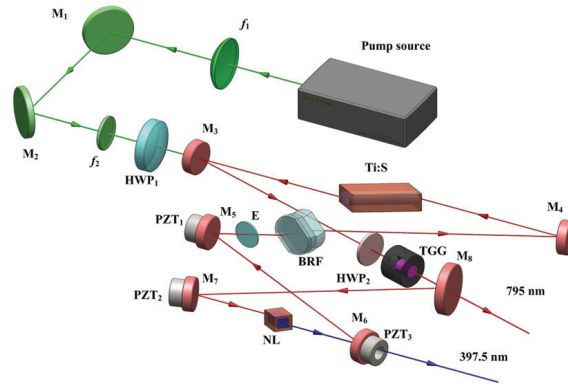


Fig. 1. Schematic diagram of the continuous frequency-tuning Ti:S laser.

the BRF or etalon is given by

$$\frac{1}{\Delta\nu_{eff}^2} = \frac{1}{\Delta\nu_L} + \frac{f^2}{(FSR)^2(\eta+L)} \quad (2)$$

where f and FSR are the finesse and free spectra range of the BRF or etalon, respectively, $\Delta\nu_L$ is the gain linewidth of the gain medium.

When the effective gain linewidth, linear and NL losses of the laser are ensured, we can evaluate the maximal frequency-tuning range without mode-hopping. The method of introducing the NL loss to a fundamental-wave resonator is a simple way to obtain a continuous frequency-tuning laser. Although, the mode-selector such as the BRF or Etalon is placed in the resonant cavity, it isn't necessary to lock their transmission peak to the frequency of the oscillating laser when the laser frequency is continuously scanned.

3. Cavity design

According to the above theoretical analysis, we design and build up an all-solid-state Ti:S laser. The configuration of the presented all-solid-state continuous frequency-tuning Ti:S laser is shown in Fig. 1. The pump source is a single-frequency and frequency-doubled Nd:YVO₄ laser with a maximal 12 W power of the green laser (F-VIII B, Yuguang Co., Ltd). The pump green laser leaded by M₁ and M₂ is coupled into the resonant cavity of the Ti:S laser by a coupling system formed with f_1 ($f=200$ mm) and f_2 ($f=100$ mm). The half wave-plate (HWP₁) in front of the resonator is used for the polarization alignment of the pump laser with respect to the optical axis of the Ti:S crystal. The resonator of the Ti:S laser, which has a ring-type configuration for the prevention of spatial hole burning, is composed of two curved mirrors with a 100-mm radius of curvature (M₃ and M₄), two curved mirrors with a 50-mm radius of curvature (M₆ and M₇), a flat mirror (M₅) and another flat mirror with a 2.95% transmission at 795 nm (M₈). M₃ and M₄ are coated with high reflection (HR) films at 750-850 nm and antireflection (AR) films at 532 nm, and the folding angle at M₃ and M₄ is set to 15.8°. M₅ coated with HR films at 750-850 nm is adhered to the PZT₁ (Piezoelectric transducer). Another two curved mirrors (M₆ and M₇) adhered to PZT₂ and PZT₃ are coated with HR films at 750-850 nm and AR films near 398 nm, and the folding angle at M₆ and M₇ is set to 10°. The angles of four concave mirrors can be enough to compensate the astigmatism in the ring cavity induced by the Brewster-cut intracavity elements including Ti:S gain crystal, a three-plate birefringent filter (BRF) and an optical diode. The Brewster-angle-cut (60.4°) Ti:S crystal with a 4-mm diameter and 20-mm-length, which is 0.05 wt% doped with FOM > 275 (Factor of Merit) is

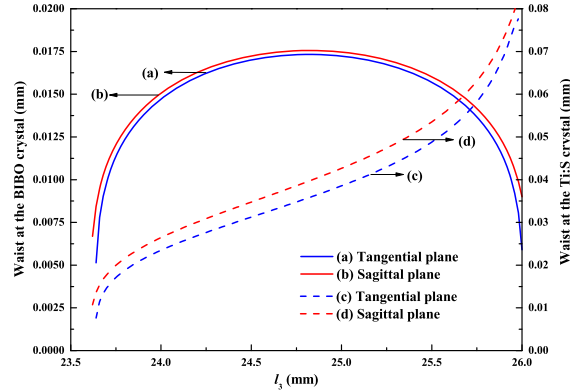


Fig. 2. Waist size at the center of the BIBO and Ti:S crystals as a function of the distance l_3 . (a) and (b), the waists at the BIBO crystal of the tangential and sagittal planes, respectively; (c) and (d), the waists at the Ti:S crystal of the tangential and sagittal planes, respectively.

mounted in a closed copper block oven cooled by water circulation and positioned between M_3 and M_4 . The three-plate BRF with thickness of 1 mm, 2 mm and 4 mm is inserted into the resonator with its Brewster incidence angle (57°) for coarsely frequency-tuning in a broad frequency-band. To enforce unidirectional oscillation, an optical diode based on the Faraday effect is used. It comprises a Brewster-cut, 3-mm long, terbium gallium garnet (TGG) Faraday crystal placed inside a stack of permanent Sm-Co ring magnets. A thin quartz plate (its function amounts to a HWP, HWP_2) is used to compensate, via optical activity, the polarization rotation induced by the TGG crystal.

A type-I phase-matched BIBO (Bismuth Triborate, BiB_3O_6) crystal is employed as the NL crystal, which can introduce a NL loss via the SHG. The BIBO crystal, which belongs to the monoclinic borate family and has a much higher NL coefficient than that of LBO (Lithium Triborate, LiB_3O_5). Considering the output power of the fundamental-wave laser and the loss induced by the crystal facets as well as the etalon effect, a relatively shorter Brewster-angle-cut (61.4°) BIBO crystal with dimensions of $3 \text{ mm} \times 3 \text{ mm} \times 5 \text{ mm}$ is utilized in our laser system, and it is cut on type-I critically phase-matched angle that is $\theta = 150.7^\circ$ and $\Phi = 90^\circ$. The crystal is wrapped with an indium foil and mounted in a temperature-controlled copper oven. Using a thermoelectrical temperature controller with accuracy of 0.03 K, the temperature of the BIBO crystal is stabilized to the optimal value of 300 K.

The total round-trip distance of the resonator is about 700 mm. To achieve a high optical to optical conversion efficiency, the pumping-to-oscillating mode matching is very important. Using the ABCD matrix formalism for paraxial ray propagation, the waist size of the oscillating mode in the centre of the Ti:S (ω_0) and the BIBO (ω_1) crystals at the tangential and sagittal planes as functions of the distance (l_3) between the M_6 or M_7 with the end-faces of the BIBO crystal for a constant distance ($l_1=48 \text{ mm}$) between M_3 or M_4 with the end-faces of the Ti:S crystal are shown in Fig. 2. According to Fig. 2, the spacing of M_6 and M_7 (l_3) is set to the center of the resonator stability region. When the astigmatism is compensated, the waists at the center of Ti:S and BIBO crystal are formed to be about $39.35 \mu\text{m}$ (sagittal plane) \times $35.48 \mu\text{m}$ (tangential plane) and $17.56 \mu\text{m}$ (sagittal plane) \times $17.33 \mu\text{m}$ (tangential plane), respectively. According to the requirement of the optimal pumping to oscillating mode matching, the waist size of the pump laser (ω_p) is adjusted to be about $24 \mu\text{m}$ by means of two lenses with focal length of 200 mm and 100 mm. Adjusting the angle of incidence on the lens of f_2 to approximately 13° compensates the astigmatism generated by the 20 mm long Ti:S laser crystal.

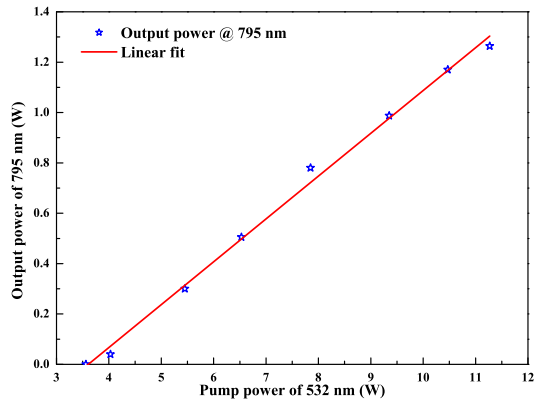


Fig. 3. Output power of Ti:S laser at 795 nm vs the pump power.

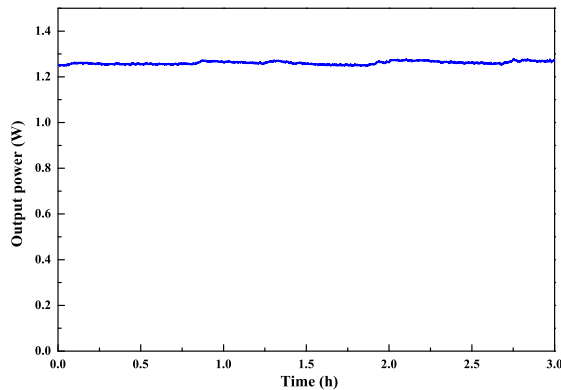


Fig. 4. Power stability of the SLM 795 nm laser.

4. Experimental results

When the NL BIBO crystal is inserted into the resonator, the SLM 795 nm laser is obtained and the function curve of the output power for the SLM 795 nm laser versus the pump power is plotted in Fig. 3. The maximum output power of 1.27 W of 795 nm is measured under the pump power of 11.27 W with the threshold pump power of 3.56 W and the slope efficiency of 16.5%. At the same time, about 90 mW of 397.5 nm is obtained owing to the SHG of the BIBO crystal. The measured long-term power stability is better than $\pm 1.2\%$ (peak-to-peak) for 3 hours without mode-hopping, which is shown in Fig. 4. The beam quality of the 795 nm laser is measured by a M^2 meter (M^2 -200, Spiricon Inc.), and the measured values of M_x^2 and M_y^2 are both 1.05. The measurement result and the corresponding spatial beam profile are shown in Fig. 5 and its inset, respectively.

To evaluate the maximal frequency-tuning range of the Ti:S laser, we have to know the values of the effective gain linewidth, linear and NL losses. The round-trip cavity loss of the 4.64% is obtained by means of measuring the relaxation resonant oscillation (RRO) frequency and output power [10]. The transmission of the output coupler is 2.95%. So, the linear loss of the Ti:S laser is 7.59%. The frequency-doubling conversion efficiency of the BIBO crystal of 4.025% is obtained according to its parameters. In our laser system, the gain linewidth is mainly decided

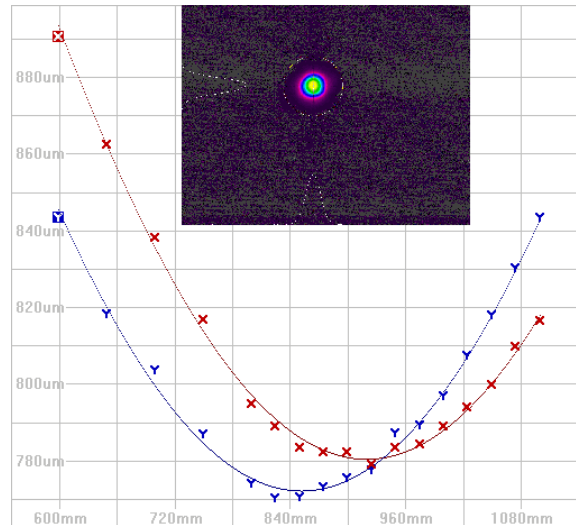


Fig. 5. Measured M^2 values and the spatial beam profile for the output laser beam of 795 nm.

by the set of the BRF which includes three silicon plates with the thickness of 1 mm, 2 mm and 4 mm. The FSR and the linewidth are 3.3×10^4 GHz and 412.5 GHz, respectively. In order to obtain the stable SLM output laser, a thin fused-quartz etalon (E) with the thickness of 0.5 mm is inserted into the resonator. The FSR and the finesse are 200 GHz and 0.6 (for uncoated fused silica), respectively. The effective linewidth with the etalon of 227 GHz is evaluated and the theoretical value of the maximal frequency-tuning range of the Ti:S laser is 67 GHz.

In the experiment, the continuous frequency-tuning range of the Ti:S laser is defined by the maximum mirrors travel that is provided by three PZT elements (PZT₁: HPS_t 150/14-10/55; PZT₂ and PZT₃: HPS_t 150/14-10/12, Piezomechanik GmbH). Considering the influences of the frequency tuning on the laser stability and the relative position of the NL BIBO crystal, the maximum travels of the PZT₂ and PZT₃ are shorter than that of the PZT₁. The PZT elements are actuated by home-made high-voltage (HV) direct current (DC) amplifier (YG-2003, Yuguang Co., Ltd) with low noise, and the output laser wavelength is recorded by a wavelength meter (WS6/765, High Finesse Laser and Electronic Systems). Before inserting the NL BIBO crystal into the resonator, a mode-hopping phenomenon will occur when the cavity length is scanned over a FSR of the laser resonator, and the maximal frequency-tuning range is one FSR of the laser resonator. After the BIBO crystal is inserted into the resonator, the frequency-tuning range of 48 GHz in the configuration of the Ti:S laser is achieved, which is shown in Fig. 6. Figure 6 gives the dependence of the laser generation frequency in the Ti:S configuration on the time during automatic frequency scanning. Modulation of the output power of the laser over the maximum possible generation frequency tuning with the help of three PZTs is less than 10.3%. On the case, the entire range of continuous tuning amounts to 48 GHz, which includes two components: the 40 GHz range provided by the PZT₁ and the 8 GHz range provided by the PZT₂ and PZT₃. Thanks to the large modulation of the output power when the cavity length is scanned, the PZT with the maximal travel over 55 μm isn't employed. But we believe that the maximal frequency-tuning range up to 67 GHz can be achieved if the PZT with larger travel is utilized. In order to reduce the long-term radiation line drift and improve the frequency stability, the Ti:S laser is locked on an extra temperature-controlled reference confocal F-P cavity with an electronic servo-system. High thermal and position stability of the reference F-P cavity leads

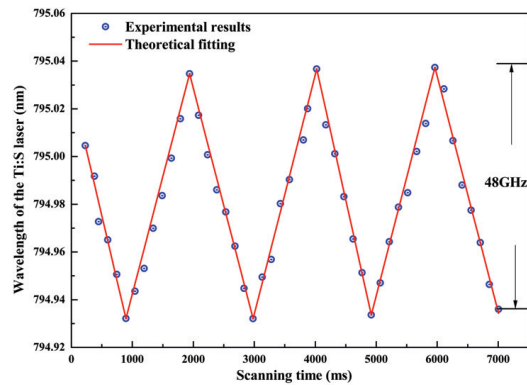


Fig. 6. Automatic smooth scanning frequency of the Ti:S laser by scanning the voltage of three PZTs.

to a reduction of long-term frequency drift of the Ti:S laser down to ± 5.5 MHz in 1 hour, which is shown in Fig. 7.

At last, we investigate the influence of the intracavity NL loss on the intensity noise of the 795 nm laser. The intensity noise is measured by means of the self-homodyne-detector which includes two silicon photo-diodes (PD, S3399). The optical signals detected by two PDs are amplified by the integrated amplifiers (CLC425) and then the amplified photo currents of two PDs are combined with a negative or positive power combiner (+/-). The sum and the subtract photocurrents stand for the intensity noise and the corresponding quantum noise limit (QNL), respectively. Finally, the noise spectra of the sum (subtract) photo currents are analyzed by a spectral analyzer with the resolution bandwidth (RBW) of 100 kHz and the video bandwidth (VBW) of 100 Hz. Figure 8 shows the measured intensity noise of the 795 nm laser without (a) and with (b) the intracavity NL crystal, respectively. Before inserting the NL crystal into the resonator, the frequency and the magnitude of the RRO for 795 nm laser are 550 kHz and 45.8 dB above the QNL. At lower frequencies from 0.2 MHz-0.4 MHz, the intensity noise level of the 795 nm laser is about 41 dB, which transmitted from the pump source. The intensity noise of the 795 nm laser reaches the QNL almost at the 2.75 MHz. After the NL crystal is inserted into the resonator, the intensity noise at the lower and the RRO frequencies are suppressed about 8 dB and 13 dB, respectively.

5. Conclusions

In summary, we have investigated the function of the NL loss on the continuous frequency-tuning characteristic and the intensity noise of the Ti:S laser. For the first time, we realized a single-frequency and continuous frequency-tuning 795 nm laser without any etalon-locking. The threshold of the Ti:S laser was 3.56 W, and the maximum output power of 1.27 W was measured under the pump power of 11.27 W with the slope efficiency of 16.5%. When the NL crystal was inserted into the cavity, the continuous frequency-tuning range of 48 GHz without mode-hopping was achieved. The NL crystal can also successfully suppress the intensity noise at and below the RRO frequencies for 13 dB and 8 dB, respectively. The obtained single-frequency Ti:S laser with continuous frequency-tuning and low intensity noise can be used in the atomic physics, quantum information and so on.

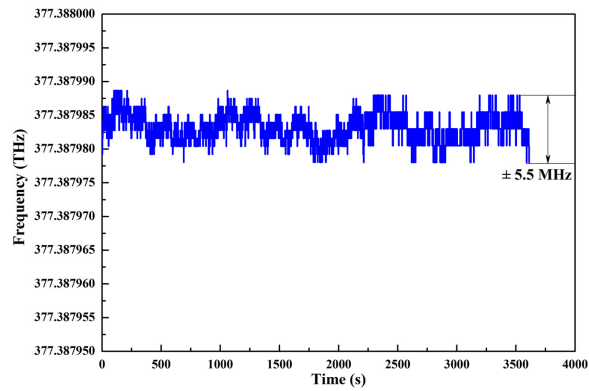


Fig. 7. Frequency drift of the locked Ti:S laser in one hour.

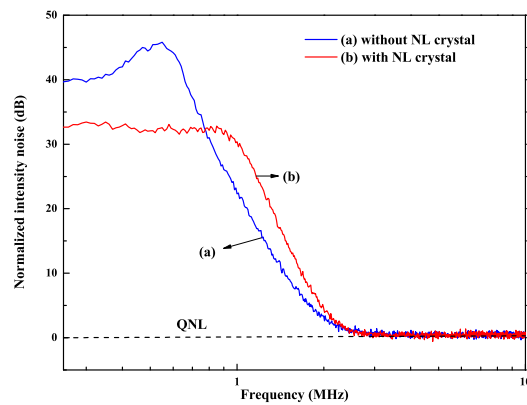


Fig. 8. Intensity noise of the laser without (a) and with (b) the NL crystal.

Acknowledgments

This research was supported in part by the National Natural Science Foundation of China (Grant No. 61405107, 61227902, 61227015), Natural Science Foundation of Shanxi Province (Grant No. 2014021011-3) and Scientific and Technological Innovation Programs of Higher Education Institutions in Shanxi (Grant No. 2013104).